Tetrahedron 70 (2014) 380–391

Contents lists available at ScienceDirect

Tetrahedron

journal homepage: www.elsevier.com/locate/tet

Nucleoside and oligonucleotide pyrene conjugates with 1,2,3-triazolyl or ethynyl linkers: synthesis, duplex stability, and fluorescence changes generated by the DNA-dye connector

Sachin A. Ingale [a,b], Frank Seela [a,b,*]

[a] Laboratory of Bioorganic Chemistry and Chemical Biology, Center for Nanotechnology, Heisenbergstraße 11, 48149 Münster, Germany
[b] Laboratorium für Organische und Bioorganische Chemie, Institut für Chemie neuer Materialien, Universität Osnabrück, Barbarastraße 7, 49069 Osnabrück, Germany

ARTICLE INFO

Article history:
Received 1 October 2013
Received in revised form 13 November 2013
Accepted 16 November 2013
Available online 21 November 2013

Keywords:
Nucleosides
DNA
Pyrene linker
Fluorescence
Duplex stability

ABSTRACT

Fluorescent nucleosides and oligonucleotides functionalized with pyrene were synthesized using 'click' chemistry or the *Sonogashira* cross-coupling reaction. The dye was connected to position-7 of 7-deaza-2′-deoxyguanosine or to the 2′-deoxyribofuranose moiety. Four different DNA-dye connectors with 1,2,3-triazolyl residues or triple bonds were constructed. Phosphoramidites of the pyrene conjugates (**9**, **14**, **25**) were prepared and used in solid-phase synthesis. Short linkers (**2**, **4**) destabilize DNA, while long linkers (**1**) increased duplex stability. Nucleosides and oligonucleotides with single dye incorporations show linker dependent fluorescence. Linker dependent excimer emission with pyrenes in proximal positions was also observed. A 'superchromophore' formed by the 7-deaza-2′-deoxyguanosine ethynylpyrene conjugate shows strong red shifted fluorescence emission at 495 nm.

1. Introduction

Pyrene is a polycyclic aromatic molecule showing monomer and excimer fluorescence.[1] Its fluorescence is sensitive to the microenvironment,[2] and excited state dimers (excimers)[3,4] are formed when pyrene residues are in a proximal position of about 10 Å distance. Pyrene has been attached as fluorescence probe to biomolecules such as proteins,[5] lipids,[6] and nucleic acids.[7,8] Pyrene–DNA conjugates have found wide-spread application in chemistry, biology, and nanotechnology.[7–9] As an example, the chain orientation of DNA (parallel or antiparallel) was verified by pyrene excimer fluorescence.[10] As the surface area of the pyrene moiety (~184 Å^2) is similar to that of an adenine–thymine Watson–Crick base pair (~184 Å^2),[11] pyrene has the propensity to intercalate into DNA causing helix stabilization.[8a,12]

Recently, our laboratory and others reported on the duplex stability and nucleobase controlled fluorescence quenching of pyrene modified nucleosides and oligonucleotides.[13–15] Furthermore, it was recognized that the attachment position between the pyrene moiety and the nucleoside (sugar residue or nucleobase) is of utmost importance for pyrene fluorescence. For an in-depth understanding of the photophysical properties of pyrene and pyrene conjugates, the reader is referred to a number of excellent reviews.[4,8a,16]

Among the various pyrene DNA attachment sites, the 5-position of pyrimidines[15,17,18] and the 7-position of 7-deazapurines[13,19] are favored as in these cases, the dye is well accommodated in the major groove of duplex DNA (purine numbering is used throughout the discussion section). Nevertheless, while various pyrene DNA attachment sites were studied with regard to monomer and excimer fluorescence, the influence of linker units in an identical environment of the DNA helix (same position and having identical nearest neighbors) is barely studied.

In this work, different linker units connecting pyrene residues have been studied in an identical environment of single-stranded and double-stranded DNA (Fig. 1). The linker does not only control the distance between the monomeric pyrene unit and the DNA helix, it also regulates the capability of the dye to form excited pyrene dimers. Therefore, particular attention was paid to the influence of the linkers on the monomeric versus excimer fluorescence in single-stranded and duplex DNA. 7-Deaza-2′-deoxyguanosine (c^7G_d) was selected as nucleobase surrogate. The linker units constitute either a 1,2,3-triazole residue or a triple bond. Pyrene was always

* Corresponding author. Tel.: +49 (0)251 53 406 500; fax: +49 (0)251 53 406 857; e-mail address: Frank.Seela@uni-osnabrueck.de (F. Seela).
URL: http://www.seela.net

0040-4020/$ – see front matter © 2013 Elsevier Ltd. All rights reserved.
http://dx.doi.org/10.1016/j.tet.2013.11.048

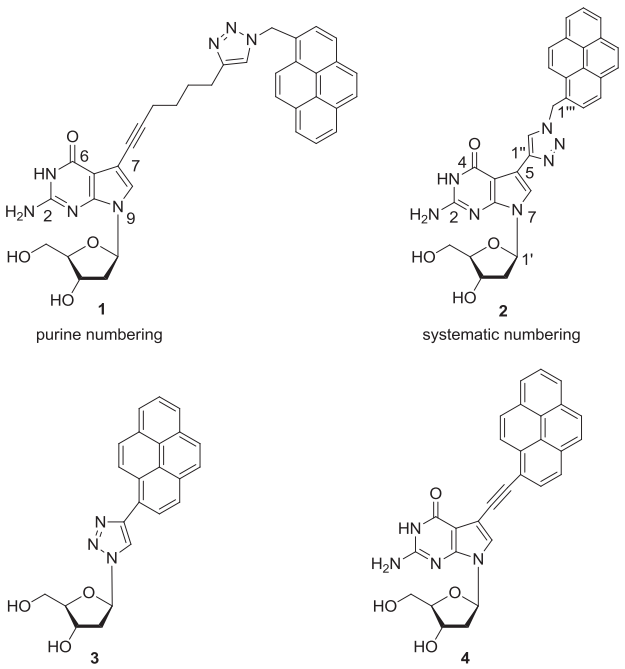

Fig. 1. Structures of nucleoside pyrene conjugates.

connected to the 7-position of c^7G_d, and dye functionalization was performed by the *Huisgen–Meldal–Sharpless*[20] 'click reaction' or *Sonogashira* cross-coupling. For the solid-phase synthesis of fluorescent oligonucleotides, phosphoramidites of the nucleoside or sugar pyrene conjugates **1**–**4** were synthesized.

2. Results and discussion

For our study, four different nucleoside pyrene conjugates and their building blocks bearing 1,2,3-triazolyl or ethynyl linkers were prepared. Nucleoside pyrene click conjugates **1**–**3** were synthesized by the copper(I)-catalyzed azide–alkyne cycloaddition (CuAAC, click chemistry), whereas ethynylpyrene conjugate **4** was synthesized by the *Sonogashira* cross-coupling reaction. The octadiynyl nucleoside pyrene click conjugate **1** was prepared according to an earlier reported procedure.[13]

2.1. Synthesis of nucleoside pyrene conjugates and phosphoramidites

2.1.1. Synthesis of pyrene conjugates containing a 1,2,3-triazolyl moiety. Nucleoside pyrene conjugate **2** was prepared from 7-ethynyl-7-deaza-2′-deoxyguanosine (**5**)[21] and 1-azidomethylpyrene (**6**)[22] in the presence of $CuSO_4 \cdot 5H_2O$ and sodium ascorbate in a 3:1:1 mixture of THF/*t*-BuOH/H_2O employing click chemistry (66% yield). For solubility reasons (THF/H_2O/*t*-BuOH), the protected (isobutyryl and DMTr) ethynylated nucleoside **7**[21b] was used as starting material for the synthesis of phosphoramidite building block **9**. The click reaction of nucleoside **7** with **6** in the presence of copper(I) gave **8** (68% yield), and subsequent phosphitylation afforded phosphoramidite **9** in 64% (Scheme 1).

The CuAAC reaction was also used for the synthesis of the abasic pyrene click conjugate **3** employing the toluoyl protected β-azide **10**[23a] and commercially available 1-ethynylpyrene (**11**) to afford the protected pyrene click conjugate **12** (83% yield).[23b] Deprotection of the toluoyl groups with 1 M sodium methoxide in methanol gave pyrene conjugate **3** in 90% yield (Scheme 2). Then, nucleoside pyrene click conjugate **3** was treated with DMTr–Cl in pyridine affording the 5′-*O*-DMTr derivative **13**. Phosphitylation of **13** gave the corresponding phosphoramidite **14** in 76% yield (Scheme 2).

2.1.2. Synthesis of pyrene conjugates with an ethynyl linker. 7-Iodo-7-deaza-2′-deoxyguanosine (**20**)[24] has already been used as key intermediate for the synthesis of various nucleoside derivatives of 7-deazaguanine (including alkynyl nucleosides **5** and **26**; for formulas see Table 1) prepared by coupling reactions (*Sonogashira*, *Stille*, *Heck*).[25] The synthesis of **20**—the starting material for **4** and **23**—suffers from an unsatisfying yield.[24,26] Consequently, a new synthesis of **20** and its DMTr derivative **23**[27] was developed.

Nucleoside **17** was prepared from 6-chloro-7-deazaguanine (**15**)[28] and the chloro sugar **16**[29] by nucleobase anion glycosylation (76% yield).[30] Isobutyrylation of **17** and subsequent selective iodination afforded nucleoside **18** (91% yield over two steps).[31] Deprotection and concomitant conversion of the 6-chloro group of **18** in sodium methoxide in methanol yielded **19**[32] (93% yield), which was demethylated (→**20**, 91%). The overall yield from **15**→**20** is 59%. Earlier yields amounted to 38–40%.[24,26] *Sonogashira* cross-coupling on **20** with 1-ethynylpyrene (**11**) afforded the nucleoside pyrene conjugate **4** (69% yield).

The intermediate **18** was also used for the synthesis of DMTr derivative **23** (Scheme 3). Displacement of the chloro substituent of protected **18** with pyrimidine-2-carboxaldoxime restored the 7-deazaguanine moiety to give compound **21** (92% yield). Selective deprotection (→**22**; 90% yield) followed by DMTr protection afforded **23** in 91% yield.[27] The overall yield of **23** starting from compound **15** is 52%. This constitutes a considerable improvement of an earlier protocol of our laboratory (**15**→**23**, overall yield 32%).[24,27] Palladium-catalyzed *Sonogashira* cross-coupling reaction of nucleoside **23** with 1-ethynylpyrene (**11**) afforded nucleoside **24**, which was then converted into phosphoramidite **25** under standard conditions (72% yield).

All new compounds were characterized by elemental analysis or mass spectroscopy, ^1H, ^{13}C, and $^1H-^{13}C$ gated-decoupled as well as DEPT-135 NMR spectra (for spectra see Figs. S6–S56, Supplementary data). The ^{13}C NMR chemical shifts are listed in Table 2 and were assigned by $^1H-^{13}C$ coupling constants (Table S1, Supplementary data) and DEPT-135 NMR spectra.

2.2. Synthesis and duplex stability of oligonucleotide pyrene conjugates

To evaluate the effect of different pyrene linkers on duplex stability and fluorescence properties, oligonucleotides were prepared by solid-phase synthesis using standard phosphoramidites and the modified building blocks **9**, **14**, and **25** (for details see the Experimental section). For this, a set of modified 12-*mer* oligonucleotides (ODNs) were synthesized by replacing dG residues (one or two) by nucleoside pyrene derivatives **1**–**4** within various positions of the complementary reference duplex 5′-d(TAG GTC AAT ACT)-3′ (**27**) and 5′-d(AGT ATT GAC CTA)-3′ (**28**). After cleavage from the solid-support and deprotection under standard conditions, the oligonucleotides were purified by RP-18 HPLC before and after detritylation. The oligonucleotide pyrene conjugates containing the long octadiynyl linker (**1**) were prepared by post-synthetic click modification using an earlier reported protocol.[13] The masses of the pyrene oligonucleotide conjugates were confirmed by MALDI-TOF mass spectrometry (Table S2, Supplementary data). For the HPLC profiles of the purified pyrene oligonucleotide conjugates see Fig. S1 (Supplementary data).

To study the impact of alkynyl 7-deazaguanine residues and pyrene conjugates on duplex stability, thermal melting (T_m) experiments were performed. The replacement of one dG residue by

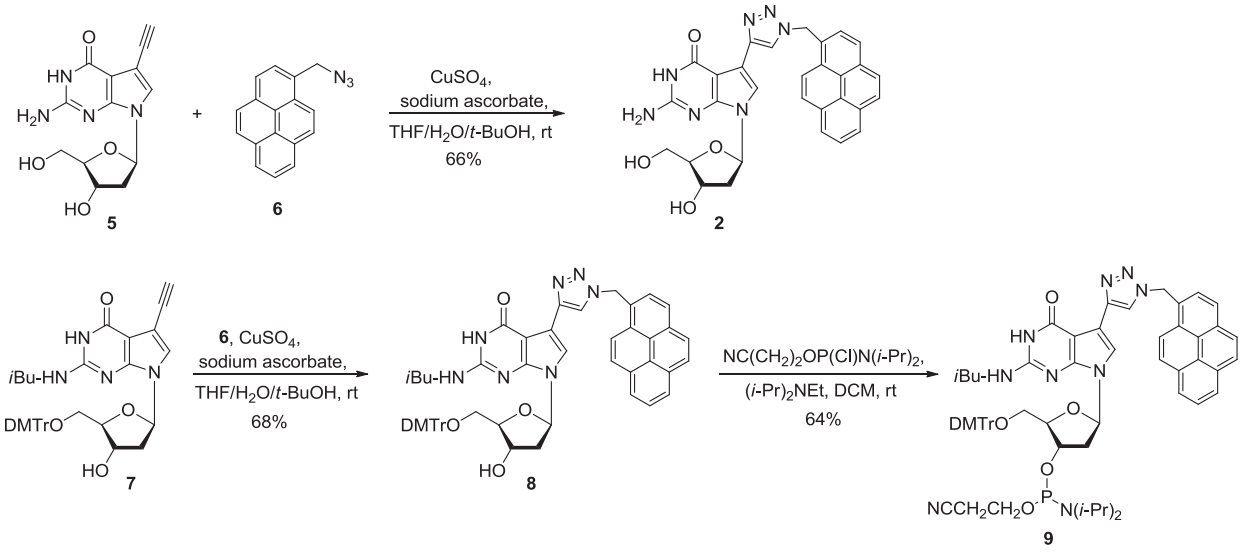

Scheme 1. Synthesis of pyrene conjugate **2** and its phosphoramidite building block **9**.

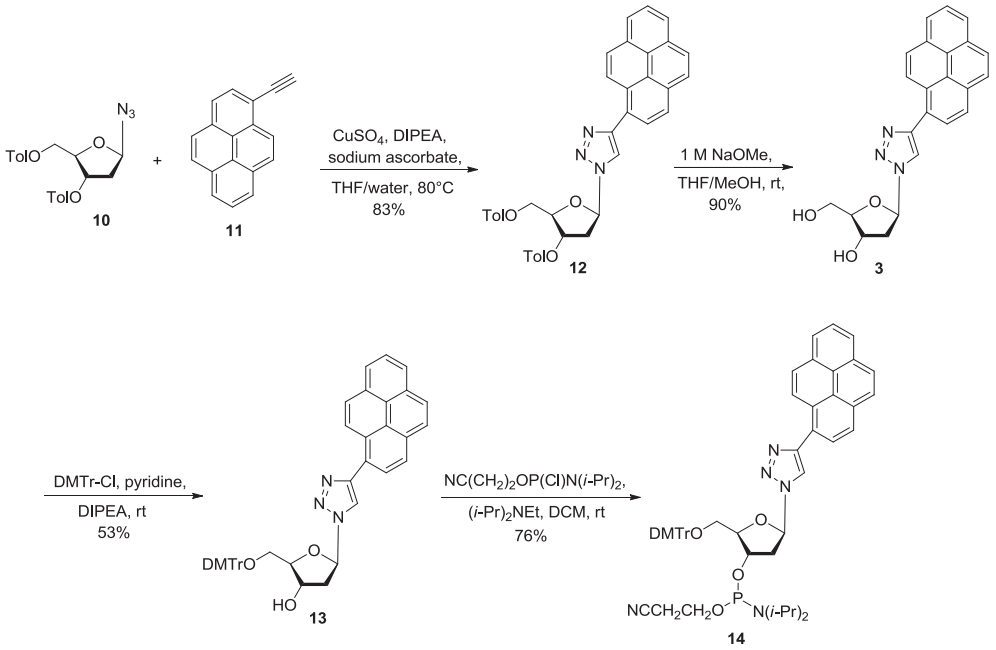

Scheme 2. Synthesis of pyrene conjugate **3** and its phosphoramidite building block **14**.

alkynyl residue **5** or **26** or by the octadiynyl pyrene conjugate **1** increases the T_m value of the duplexes compared to that of the unmodified reference duplex **27**·**28**. On the contrary, incorporation of pyrene conjugates **2**–**4** slightly decreases the thermal stability compared to the reference duplex (Table 1). From that the following conclusions can be drawn: (i) alkynyl residues (short and long) have a positive effect on duplex stability; (ii) incorporation of octadiynyl pyrene click conjugate **1** increases the duplex stability, while pyrene conjugates **2**–**4** decrease the stability; (iii) two consecutive incorporations of pyrene conjugates **2**–**4** strongly decrease the T_m value compared to only one incorporation; (iv) incorporation of pyrene derivatives at the center of the duplex always gives the most pronounced destabilization compared to incorporations at the terminus of the duplex; (v) the thermal stability of duplexes incorporating **1**–**4** decreases in the following order: octadiynyl pyrene click conjugate (**1**)>abasic click conjugate (**3**)≥ ethynylpyrene click conjugate (**2**)>ethynylpyrene conjugate (**4**).

2.3. Influence of linkers on the photophysical properties of nucleoside and oligonucleotide pyrene conjugates

To evaluate the influence of the different linker units on the photophysical properties of pyrene conjugates, UV–vis and fluorescence spectra of pyrene conjugates **1**–**4**, single-stranded (ss) ODNs and corresponding duplexes (ds) containing **1**–**4** were measured. In compounds **1**, **2**, and **4**, the dye is connected to a 7-deazaguanine base, while compound **3** contains an abasic moiety. For all measurements, identical concentrations of the nucleoside pyrene conjugates (4 μM) and oligonucleotide pyrene conjugates (2 μM) were used (for details see the Experimental section).

Various effects of the linker units on the pyrene fluorescence have to be considered. (i) The length of the linker (long/short) affects the spatial arrangement of the dye with respect to the DNA helix, e.g., the positioning within the DNA groove. The linker length might also enforce or restrict intercalation of pyrene between the base

Table 1
T_m values of modified duplexes[a]

Duplexes	T_m [°C]	ΔT_m[b] [°C]	Duplexes	T_m [°C]	ΔT_m[b] [°C]
5′-d(TAG GTC AAT ACT) (**27**) 3′-d(ATC CAG TTA TGA) (**28**)	50	—	5′-d(TAG GTC AAT ACT) (**27**) 3′-d(ATC CAG TTA TGA) (**28**)	50	—
5′-d(TA**26** GTC AAT ACT) (**29**) 3′-d(ATC CAG TTA TGA) (**28**)	52[c]	+2	5′-d(TA**1** GTC AAT ACT) (**32**) 3′-d(ATC CAG TTA TGA) (**28**)	54[d]	+4
5′-d(TAG GTC AAT ACT) (**27**) 3′-d(ATC CA**26** TTA TGA) (**30**)	51[c]	+1	5′-d(TAG GTC AAT ACT) (**27**) 3′-d(ATC CA**1** TTA TGA) (**33**)	55[d]	+5
5′-d(TA**26 26**TC AAT ACT) (**31**) 3′-d(ATC CAG TTA TGA) (**28**)	53[c]	+3	5′-d(TA**1 1**TC AAT ACT) (**34**) 3′-d(ATC CAG TTA TGA) (**28**)	50[d]	0
5′-d(TA**5** GTC AAT ACT) (**35**)[e] 3′-d(ATC CAG TTA TGA) (**28**)	54	+4	5′-d(TA**2** GTC AAT ACT) (**38**) 3′-d(ATC CAG TTA TGA) (**28**)	49	−1
5′-d(TAG GTC AAT ACT) (**27**) 3′-d(ATC CA**5** TTA TGA) (**36**)[e]	54	+4	5′-d(TAG GTC AAT ACT) (**27**) 3′-d(ATC CA**2** TTA TGA) (**39**)	45	−5
5′-d(TA**5 5**TC AAT ACT) (**37**)[e] 3′-d(ATC CAG TTA TGA) (**28**)	55	+5	5′-d(TA**2 2**TC AAT ACT) (**40**) 3′-d(ATC CAG TTA TGA) (**28**)	39	−11
5′-d(TA**4** GTC AAT ACT) (**44**) 3′-d(ATC CAG TTA TGA) (**28**)	46	−4	5′-d(TA**3** GTC AAT ACT) (**41**) 3′-d(ATC CAG TTA TGA) (**28**)	49	−1
5′-d(TAG GTC AAT ACT) (**27**) 3′-d(ATC CA**4** TTA TGA) (**45**)	40	−10	5′-d(TAG GTC AAT ACT) (**27**) 3′-d(ATC CA**3** TTA TGA) (**42**)	48	−2
5′-d(TA**4 4** TC AAT ACT) (**46**) 3′-d(ATC CAG TTA TGA) (**28**)	42	−8	5′-d(TA**3 3**TC AAT ACT) (**43**) 3′-d(ATC CAG TTA TGA) (**28**)	37	−13

[a] Measured at 260 nm in 1 M NaCl, 100 mM $MgCl_2$, and 60 mM Na-cacodylate (pH 7.0) with 5 μM+5 μM single-strand concentration.
[b] Refers to the temperature difference of the modified duplex versus the unmodified reference duplex.
[c] Ref. 25a.
[d] Ref. 13.
[e] Ref. 21b.

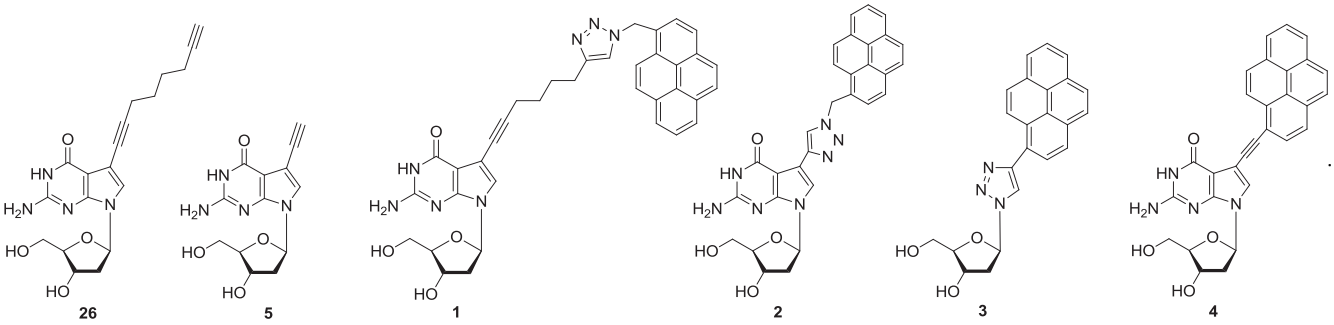

pairs. (ii) A long, flexible linker gives the dye the freedom of motion, while motion is restricted by a more rigid and short linker. (iii) The linker units can change the electronic properties of the fluorophore by π-electron interactions. (iv) Hydrophobic or hydrophilic linkers as well as charges (positive or negative) affect the interaction with the DNA helix or surrounding water molecules or ions.

2.3.1. Monomeric 7-deazaguanine pyrene conjugates. At first, pyrene conjugates **1**–**4** were characterized by UV–vis spectra (Fig. 2a) measured in methanol. The absorbance spectrum of ethynylpyrene conjugate **4** is significantly red shifted (48 nm) compared to those of pyrene click conjugates **1**–**3**, indicating the stronger electronic coupling between the nucleobase moiety and the attached pyrene.[17,33]

Fluorescence measurements were performed for all four pyrene conjugates (**1**–**4**) (Fig. 2b) using identical concentrations as used for the measurement of the UV–vis spectra. Based on the absorbance spectra of **1**–**3**, the excitation wavelength was chosen at the isosbestic point of 345 nm. For **4**, two excitation wavelengths were selected, namely the arbitrary excitation wavelength at 345 nm (isosbestic point of **1**–**3**) and the maximum of fluorescence at 389 nm (for the spectrum with excitation at 389 nm, see Fig. S2, Supplementary data).

The emission spectra of the 7-deaza-2′-deoxyguanosine (c^7G_d) pyrene click conjugates **1** and **2** show monomer fluorescence (maximum at 378 nm with a shoulder at 394 nm), whereas the monomer fluorescence (maximum at 388 nm with a shoulder at 401 nm) of abasic click conjugate **3** is slightly red shifted. The abasic pyrene click conjugate **3** (Φ=0.044 and brightness value=1395) shows significantly higher fluorescence intensity compared to pyrene click conjugates **1** (Φ=0.004 and brightness value=150) and **2** (Φ=0.0019 and brightness value=69). The emission spectrum of ethynylpyrene conjugate **4** (maximum at 495 nm; Φ=0.058 and brightness value=2210) is significantly red shifted (≈95 nm) compared to the other pyrene click conjugates **1**–**3**, due to strong electronic interactions between the nucleobase moiety and the attached pyrene (Fig. 2b).[17,33] A strong red shift (maximum at 480 nm) has also been observed for 8-ethynylpyrene 2′-deoxyguanosine (dG–C≡C–Py).[18e] However, this effect is much more pronounced for the 7-deazaguanine moiety.

2.3.2. Oligonucleotide pyrene conjugates. Subsequently, the photophysical properties of single-stranded and double-stranded oligonucleotides incorporating the four different pyrene linker conjugates (**1**–**4**) were studied. UV spectra indicate the presence of the pyrene residues in oligonucleotides in the range of 300–400 nm. Similar to the UV data of monomeric linker conjugates, differences are observed for single-stranded oligonucleotides and duplexes (Fig. S3, Supplementary data).

Next, fluorescence spectra of ss ODNs and their corresponding duplexes were determined (Fig. 3 and Fig. S4, Supplementary data).

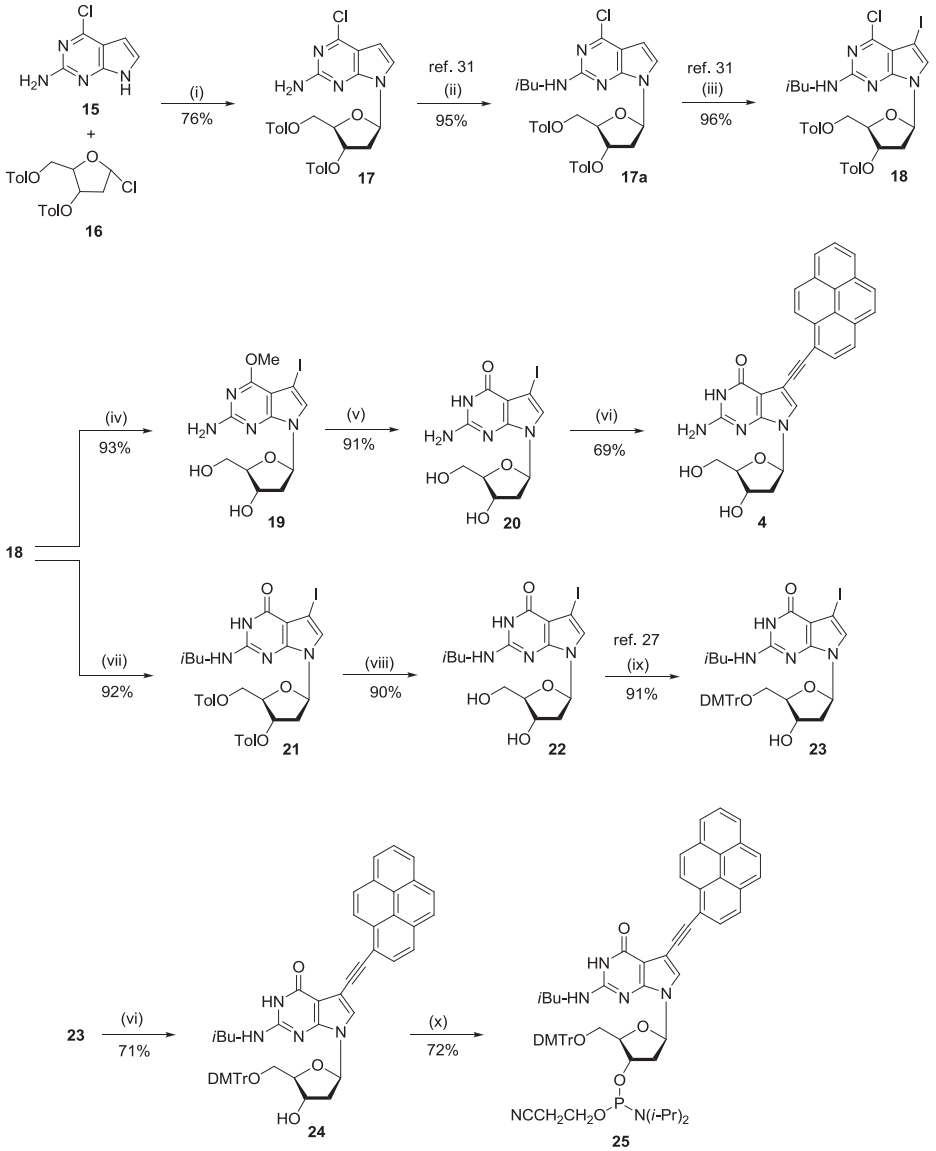

Scheme 3. Syntheses of key intermediate **20**, ethynylpyrene conjugate **4** and its phosphoramidite building block **25**. Reagents and conditions: (i) KOH, MeCN, rt; (ii) *i*-BuCl, pyridine, rt; (iii) NIS, DMF, 80 °C; (iv) 0.5 M NaOMe, reflux; (v) 2 N NaOH, reflux; (vi) 1-ethynylpyrene (**11**), Pd[$(PPh_3)_4$], CuI, anhydrous DMF, rt; (vii) pyridine-2-carboxaldoxime, 1,1,3,-tetramethylguanidine, DMF/dioxane, rt; (viii) 1 M NaOMe, THF, rt; (ix) DMTr-Cl, pyridine, rt; (x) $(i\text{-Pr})_2$NEt, $NC(CH_2)_2OP(Cl)N(i\text{-Pr})_2$, anhydrous DCM, rt.

Complementary strands were always unmodified (**27** or **28**). All ss ODNs containing single pyrene click conjugates with a triazolyl linker (**1**–**3**) as well as their duplexes show pyrene monomer fluorescence. The ethynyl linker in ss ODNs **44** and **45** and their corresponding duplexes causes a broad fluorescence band centered around 470 nm (excitation at 389 nm), which is 60 nm red shifted compared to the monomer fluorescence of linker conjugates **1**–**3** (Fig. 3d).

The linker conjugates **1**, **2**, and **4** show a decreased and conjugate **3** an increased fluorescence upon oligonucleotide duplex formation. Duplexes containing **4** show fluorescence at long wavelengths similar to nucleoside **4**. These observations made on **4** are in line with the findings for 8-ethynylpyrene 2′-deoxyguanosine (dG–C≡C–Py) and oligonucleotides containing this compound.[17,18e]

Then, the influence of the various linkers was studied on oligonucleotides incorporating two consecutive pyrene click conjugates with a triazolyl linker (**1**–**3**) in one strand. Single-stranded oligonucleotides **34**, **40**, and **43** exhibit both monomer and excimer emission bands. The excimer band is formed by intrastrand interaction of two pyrene residues (Fig. 3). Similar observations have also been made when consecutive pyrene residues were linked to the 2′-hydroxyl group of the sugar moiety or were replacing the nucleobase.[34] For **28**·**34** and **28**·**40**, the excimer fluorescence is quenched upon duplex formation compared to the ss oligonucleotides or in case of **28**·**43** fluorescence increases.

For ss ODN **46** and its corresponding duplex **28**·**46**—both containing the ethynyl linker—the expected typical shift of the pyrene excimer fluorescence is not observed. Instead, a small red shift of 23 nm was detected. This is the result of the electronic structure of the 7-ethynylpyrene c^7G_d conjugate, which forms a new fluorochromic system consisting of the 7-deazaguanine moiety and the pyrene unit. Corresponding findings have been reported by Wagenknecht[35] and others[36] for 5-ethynylpyrene dU and 8-ethynylpyrene dA conjugates forming a so-called ‘superchromophore’. The ‘excimer’ of duplex **28**·**46** shows partial charge transfer and excitation energy delocalization in the lowest excited state. Accordingly, a proximal positioning of the pyrene moieties of compound **4** leads to formation of just an ‘excimer-type’ state, in which the two nucleobases are part of the dimeric system as demonstrated by molecular dynamics simulation (Fig. 5d).

Next, we determined the monomer (M) to excimer (Ex) ratio of single-stranded and duplex DNA containing the consecutively arranged pyrene conjugates **1**–**3**. ODNs **34**, **40**, and **43** gave a very

Table 2
^{13}C NMR chemical shifts of 7-deazapurine derivatives and pyrene conjugates[a]

	C2[b]	C6[b]	C5[b]	C7[b]	C8[b]	C4[b]	Triazole	$CH/CH_2/CH_3/OCH_3$	C=O/C≡C	C1′	C2′	C3′	C4′	C5′
	C2[c]	C4[c]	C4a[c]	C5[c]	C6[c]	C7a[c]								
17[f]	159.4	154.0	108.9	100.3	122.7	151.3	—	—/—/21.1/—	165.5, 165.2/—	81.0	—[e]	75.2	82.8	64.2
17a	151.8[d]	151.5[d]	113.7	100.1	127.4	150.9[d]	—	34.5/—/19.1, 19.2, 21.1/—	174.8, 165.4, 165.2/—	84.1	35.5	75.2	81.4	64.1
18	151.6[d]	151.4[d]	112.8	54.1	132.2	151.1[d]	—	34.6/—/19.1, 19.2, 21.2/—	174.8, 165.4, 165, 2/—	83.8	35.7	75.0	81.5	64.0
19	159.4	162.8	98.7	51.7	124.1	154.1	—	—/—/—/53.0	—	82.1	—[e]	70.9	87.1	61.9
20[g]	152.7	158.1	99.8	55.0	121.7	150.5	—	—	—	82.2	—[e]	70.9	87.1	61.9
2	152.8	158.8	96.7	109.6	113.6	151.3	141.6, 122.8[d]	—/50.9/—/—	—	82.2	—[e]	71.1	87.1	62.0
4	153.5	158.2	99.6	98.7	122.2	150.7	—	—	—/90.6, 89.0	82.5	—[e]	71.0	87.3	61.9
21	155.8	147.1	104.1	56.2	123.7	147.6	—	34.5/—/18.5, 18.7, 21.0/—	179.8, 165.3, 165.0/—	82.5	35.8	74.9	81.2	63.9
22[h]	147.6	156.1	104.0	55.7	124.3	147.1	—	34.8/—/18.9, 18.8/—	180.0/—	82.6	—[e]	70.8	87.3	61.7
8	148.2[d]	156.9	100.8	110.4	115.6	147.1[d]	140.8, 123.2[d]	34.7/50.8/18.8/54.9	180.0, 158.0, 157.9/—	82.5	—[e]	70.5	85.4	64.0
24	147.9[d]	156.2	99.3	103.9	125.7[d]	147.7[d]	—	34.8/—/18.9/54.9	180.2, 158.0/89.6, 89.3	82.9	—[e]	70.5	85.7	64.1
12	—	—	—	—	—	—	146.5, 125.2[d]	—/—/21.0, 21.2/—	165.5, 165.3/—	88.1	—[e]	74.5	82.4	63.9
3	—	—	—	—	—	—	146.4, 124.8[d]	—	—	88.4[d]	—[e]	70.4	88.3[d]	61.6
13	—	—	—	—	—	—	146.4, 125.5[d]	—/—/—/54.7	—	87.9	—[e]	70.2	86.2	63.9

[a] Measured in DMSO-d_6 at 298 K.
[b] Purine numbering.
[c] Systematic numbering.
[d] Tentative.
[e] Superimposed by DMSO.
[f] Ref. 30.
[g] Ref. 24.
[h] Ref. 27.

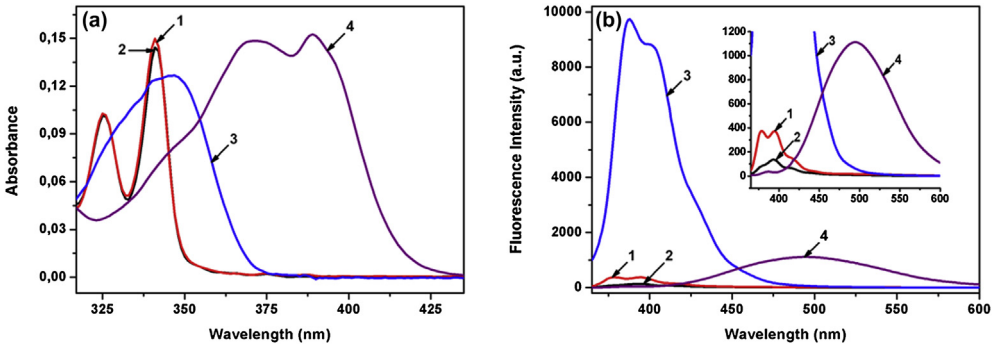

Fig. 2. (a) UV–vis absorption spectra of pyrene conjugates **1**–**4**. (b) Fluorescence spectra of pyrene conjugates **1**–**4**; inset: enlarged fluorescence spectra of conjugates **1**, **2**, and **4**. All measurements were performed in methanol (4 μM) containing 1% DMSO. Excitation wavelength: 345 nm.

low monomer to excimer ratio, i.e., 0.12, 0.08, and 0.16, respectively (Fig. 4 and Table S4, Supplementary data). The low M/Ex ratios suggest that the two pyrene residues effectively arrange themselves to form an excimer. Upon duplex formation, the monomer to excimer ratio only slightly varies (increase or decrease) for duplexes containing **2** or **3** (M/Ex=0.10 and 0.11 for **40**·**28** and **43**·**28**, respectively). This indicates that upon duplex formation the two pyrene residues are still close enough to form an excimer. In contrast, duplex **34**·**28** containing **1** with a long flexible linker unit exhibits a strongly increased monomer to excimer ratio (M/Ex=0.38) compared to M/Ex=0.12 for ss ODN **34**. This implies that upon duplex formation the two pyrene residues move slightly away from each other. This is also confirmed by the molecular dynamics simulation study (Fig. 5a).

To visualize the effect of the different linker units employed in this study, molecular dynamics simulation using AMBER force field were performed on 12-*mer* duplexes containing one or two pyrene residues (**1**–**4**) (Fig. 5 and Fig. S5, Supplementary data). The energy minimized molecular structures were built as B-type DNA. The molecular models (Fig. 5) suggest pyrene–pyrene stacking interactions in the grooves, in a similar manner as observed for DNA duplexes containing pyrene functionalized *arabino* uridine residues.[37] However, here intrastrand interactions were studied, while in the case of the pyrene *arabino* uridine conjugates interstrand interactions were evaluated.[37]

Regarding pyrene dimer formation, it is obvious that the short stiff linkers **2** and **4** lead to strong pyrene interactions (Fig. 5b,d), while the longer linker **1** (Fig. 5a) gives the pyrene residues freedom of motions thereby reducing the chance of dimer formation. This phenomenon is supported by the duplex stabilities (Table 1). The highest T_m values are found for duplexes with the long linker pyrene conjugate **1**, while stability is reduced for duplexes with the short linker derivatives (**2**, **4**). This effect is apparently caused by the bulky pyrene moieties as the corresponding derivatives with octadiynyl and ethynyl side chains always stabilize the duplex structure. When more than two consecutive pyrene residues are present in duplex DNA, the situation might change again as the pyrene interactions can compensate the destabilizing effect. Such a phenomenon has already been described by Hrdlicka and coworkers.[38] The situation for the abasic conjugate **3** is different. The triazole residues located opposite to dC cannot form base pairs by hydrogen bonds. Nevertheless, it is surprising that a single replacement of a dG residue by the abasic pyrene conjugate **3** leads to a T_m value almost as high as that of the unmodified duplex. Regarding fluorescence, the intensity decreases in duplexes compared to ss. This is valid for monomer as well as excimer emission and occurs when the pyrene is linked to the 7-deazaguanine moiety. The situation is less clear for the abasic triazole conjugates. Here, the fluorescence changes strongly depend on the position of incorporation.

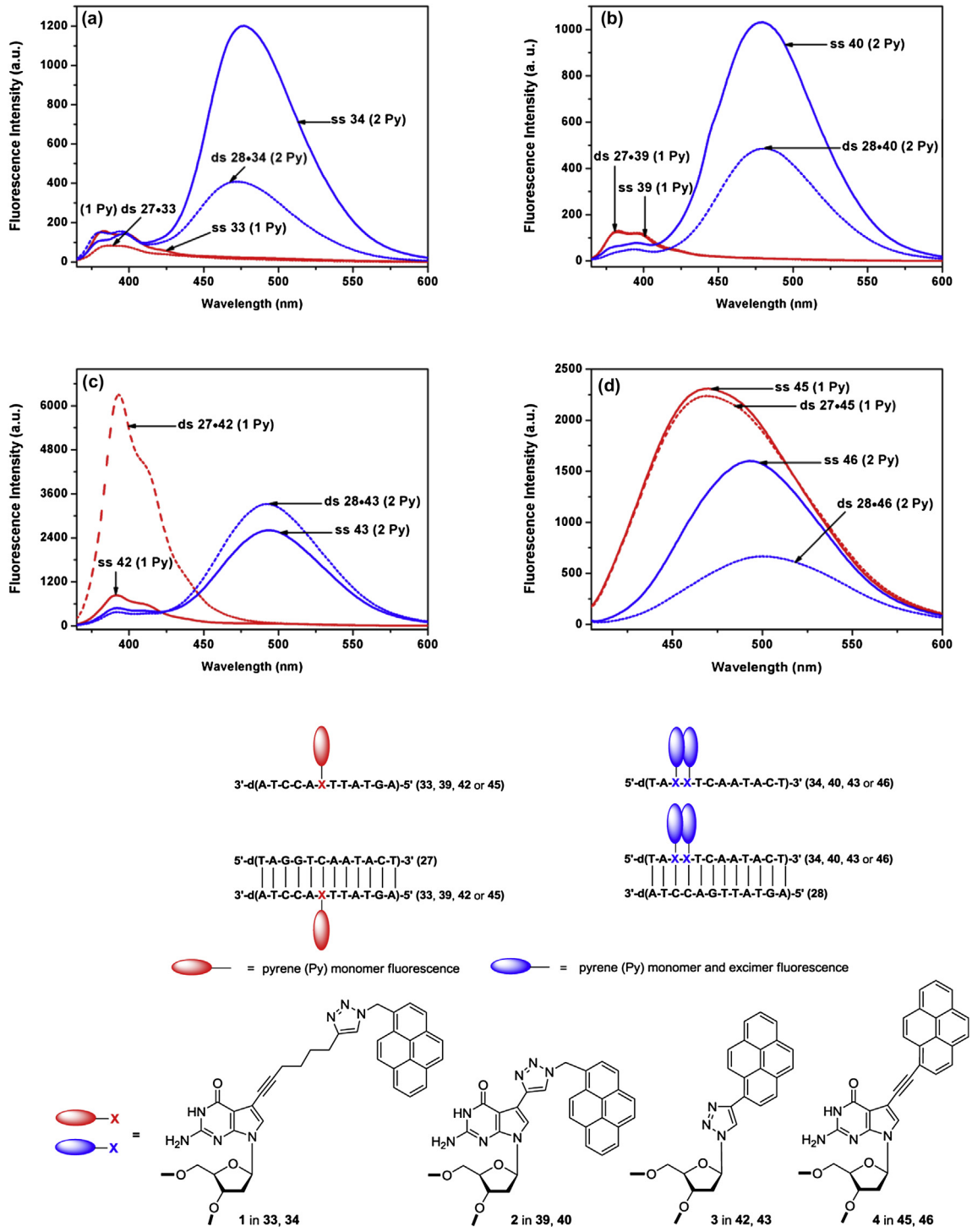

Fig. 3. Fluorescence emission spectra of 2 μM ss ODNs and corresponding ds ODNs (2 μM of each strand) measured in 1 M NaCl, 100 mM $MgCl_2$, and 60 mM Na-cacodylate buffer (pH 7.0). (a) ss ODNs **33**, **34** and ds ODNs **27**·**33**, **28**·**34**; (b) ss ODNs **39**, **40**, and ds ODNs **27**·**39**, **28**·**40**; (c) ss ODNs **42**, **43** and ds ODNs **27**·**42**, **28**·**43**; (d) ss ODNs **45**, **46** and ds ODNs **27**·**45**, **28**·**46**. Excitation at 345 nm for ss and ds ODNs with **1**–**3**. Excitation at 389 nm for ss and ds ODNs with **4**.

3. Conclusion

Fluorescent nucleoside and oligonucleotide pyrene conjugates with four different linkers were synthesized with the dye attached to the nucleobase (7-deazaguanine) or the 2′-deoxyribofuranose moiety. The linkers contain an 1,2,3-triazol residue or a triple bond. The pyrene moieties were installed by the 'click' reaction or cross-coupling on nucleosides, phosphoramidites (**9**, **14**, **25**) or oligonucleotides by post-modification. For this, a multi-step high yield synthesis of the phosphoramidite of 7-ethynylpyrene 7-deaza-2′-deoxyguanosine (**4**) was developed. The four different linker units have a very specific impact on DNA duplex stability and fluorescence. Short linkers decrease stability, while the long linker **1** has a positive stabilizing effect and gives the pyrene moiety freedom of motion.

Due to nucleobase quenching, the monomeric fluorescence of the nonbase-pairing sugar–triazol–pyrene click adduct **3** is significantly higher than those of the 7-deazaguanine adducts with

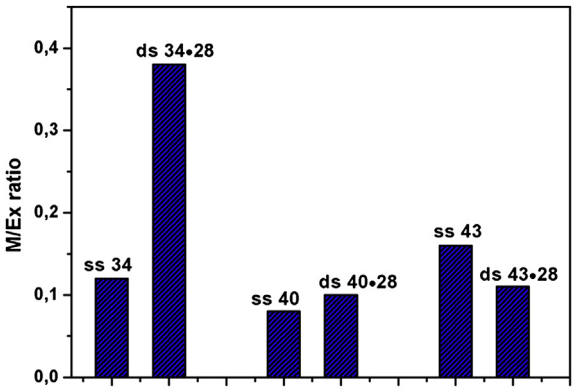

Fig. 4. Monomer to excimer fluorescence ratios of ss DNA and ds DNA containing pyrene conjugates **1**–**3**. Fluorescence emission spectra of 2 μM ss ODNs and corresponding ds ODNs (2 μM of each strand) were measured in 1 M NaCl, 100 mM $MgCl_2$, and 60 mM Na-cacodylate buffer (pH 7.0) (excitation wavelength: 345 nm). M: maximum monomer fluorescence intensity. Ex: maximum excimer fluorescence intensity.

UV spectra were recorded on a spectrophotometer: λ_{max} in nm, ε in $dm^3\ mol^{-1}\ cm^{-1}$. NMR spectra: measured at 300.15 MHz for ^1H, 75.48 MHz for ^{13}C, and 121.52 MHz for ^{31}P. The *J* values are given in hertz (Hz) and δ in parts per million (ppm). For NMR spectra recorded in DMSO, the chemical shift of the solvent peak was set to 2.50 ppm for ^1H NMR and 39.50 ppm for ^{13}C NMR. The ^{13}C NMR signals were assigned on the basis of DEPT-135 and ^1H–^{13}C gated-decoupled NMR spectra (for coupling constants see Table S1, Supplementary data). Reversed-phase HPLC was carried out on a 250×4 mm RP-18 LiChrospher 100 column with an HPLC pump connected with a variable wavelength monitor, a controller, and an integrator. Gradients used for purification of oligonucleotides by HPLC chromatography: A=MeCN; B=0.1 M (Et_3NH)OAc (pH 7.0)/MeCN, 95:5. Gradient (I): 3 min 15% A in B, 12 min 15–50% A in B, flow rate 0.8 mL min^{-1}; or 0–35 min 10–55 % A in B; gradient (II): 0–35 min 0–50% A in B, flow rate 0.8 mL min^{-1}. The molecular masses of oligonucleotide 'click' conjugates were determined by MALDI-TOF mass spectrometry in the linear positive mode with 3-

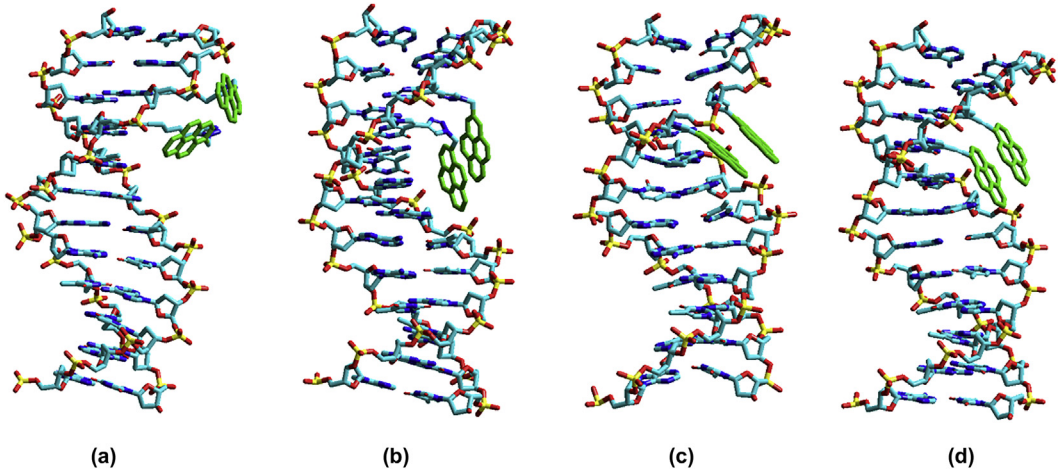

Fig. 5. Molecular models of duplex 5′-d(TA**X** **X**TC AAT ACT) ·3′-d(ATC CAG TTA TGA). (a) ds ODN **34**·**28** with X=**1**; (b) ds ODN **40**·**28** with X=**2**; (c) ds ODN **43**·**28** with X=**3** and (d) ds ODN **46**·**28** with X=**4**. The models were constructed using Hyperchem 8.0 and energy minimized using AMBER calculations.

short and long click connectors. Nucleoside **4** forms a new superchromophore consisting of the 7-deazaguanine moiety and the acetylene linked pyrene. The rigid alkyne part of an ethynyl linker places the pyrene in the major groove of duplex DNA. All ss and ds oligonucleotides with two proximal pyrenes show excimer fluorescence, but with different shifts for monomer and excimer emission (around 80 nm for triazole linked pyrenes and only 23 nm for the ethynylpyrene 7-deazaguanine superchromophore).

Different to other ethynylpyrene conjugates, namely 5-ethynylpyrene dU and dC or 8-ethynylpyrene dA and dG,[17] the monomer and excimer emission of **4** is significantly red shifted for the monomer fluorescence and for the 'excimer-type' fluorescence (adjacent superchromophores) in single-stranded and double-stranded oligonucleotides.

4. Experimental section

4.1. General materials and methods

All chemicals and solvents were of laboratory grade as obtained from commercial suppliers and were used without further purification. Thin layer chromatography (TLC) was performed on TLC aluminum sheets covered with silica gel 60 F_{254} (0.2 mm). Flash column chromatography (FC): silica gel 60 (40–60 μM) at 0.4 bar.

hydroxypicolinic acid (3-HPA) as a matrix (Table S2, Supplementary data). The thermal melting curves were measured with an UV–vis spectrophotometer equipped with a thermoelectrical controller. The temperature was measured continuously in the reference cell with a Pt-100 resistor with a heating rate of 1 °C min^{-1}.

4.2. Fluorescence measurements performed on nucleoside and oligonucleotide pyrene conjugates

Fluorescence spectra of all nucleoside pyrene conjugates (**1**–**4**) were measured in methanol (for solubility reasons all 'click' conjugates were first dissolved in 1% of DMSO and then diluted with methanol, 99%). All measurements were performed with identical concentrations, i.e., 4 μM. Fluorescence spectra of ss oligonucleotide pyrene conjugates and their duplexes were measured in 1 M NaCl, 100 mM $MgCl_2$, and 60 mM Na-cacodylate buffer (pH 7.0). All measurements were performed with identical concentrations, i.e., 2 μM for ss oligonucleotides and 2 μM+2 μM for ds oligonucleotides. Excitation wavelengths of 345 nm and 389 nm were used.

The fluorescence quantum yields, Φ, of pyrene conjugates were determined by using quinine sulfate in sulfuric acid (0.1 N) as a standard with a known Φ of 0.55. The brightness value of pyrene conjugates were calculated as: brightness=ε_{max} Φ (see Table S3, Supplementary data).

4.3. Synthesis, purification, and characterization of oligonucleotides

The oligonucleotide syntheses were performed on a DNA synthesizer at 1 μmol scale (trityl-on mode) employing the standard phosphoramidites and the modified building blocks **9**, **14** as well as **25**, following the synthesis protocol for 3′-cyanoethyl phosphoramidites. The average coupling yield was always higher than 95%. After cleavage from the solid-support, the oligonucleotides were deprotected in 28% aq NH_3 for 16 h at 60 °C. The DMT-containing oligonucleotides were purified by reversed-phase HPLC (RP-18) with the gradient I. Then, the mixture was evaporated to dryness, and the residue was treated with 2.5% $Cl_2CHCOOH/CH_2Cl_2$ for 2 min at 0 °C to remove the 4,4′-dimethoxytrityl residues. The detritylated oligomers were purified by reversed-phase HPLC with the gradient II. The oligomers were desalted on a short column (RP-18, silica gel) using H_2O for elution of the salt, while the oligomers were eluted with MeOH/H_2O (3:2). The oligonucleotides were lyophilized on a Speed Vac evaporator to yield colorless solids, which were stored frozen at −24 °C. The extinction coefficients ε_{260} (H_2O) of the nucleosides are: dA 15,400, dG 11,700, dT 8800, dC 7300, **1** 26,000, **2** 24,500 (MeOH), **3** 16,100 (MeOH) and **4** 26,200 (MeOH).

4.4. 2-Amino-7-(2-deoxy-β-D-*erythro*-pentofuranosyl)-3,7-dihydro-5-[1-(pyrenmethyl)-1*H*-1,2,3-triazol-4-yl]-4*H*-pyrrolo [2,3-*d*]pyrimidin-4-one (2)

To a solution of **5**[21] (0.09 g, 0.31 mmol) and 1-azidomethylpyrene[22] (0.112 g, 0.43 mmol) in THF/H_2O/*t*-BuOH (3:1:1, 5 mL), sodium ascorbate (0.31 mL, 0.31 mmol) of a freshly prepared 1 M solution in water and copper(II) sulfate pentahydrate 7.5% in water (0.26 mL, 0.08 mmol) were added. The reaction mixture was stirred vigorously in the dark at room temperature and was monitored by TLC. After completion of the reaction, the solvent was evaporated, and the residue was purified by FC (silica gel, column 10 cm×3 cm, CH_2Cl_2/MeOH, 93:7) to give **2** as a colorless solid (0.112 g, 66%). TLC (CH_2Cl_2/MeOH, 90:10): R_f 0.23; λ_{max} (MeOH)/nm 260 (ε/dm^3 mol^{-1} cm^{-1} 24,500), 264 (30,100), 275 (41,200), 311 (15,000), 325 (25,300), 341 (36,100). ^{1}H NMR (DMSO-d_6, 300 MHz) (δ, ppm): 2.04–2.11 (m, 1H, H$_\alpha$-2′), 2.32–2.41 (m, 1H, H$_\beta$-2′), 3.50–3.53 (m, 2H, 2×H-5′), 3.76–3.77 (m, 1H, H-4′), 4.30–4.31 (m, 1H, H-3′), 4.94 (t, *J*=5.4 Hz, 1H, HO-5′), 5.23 (d, *J*=3.6 Hz, 1H, HO-3′), 6.31–6.43 (m, 3H, H-1′, NH_2), 7.46 (s, 1H, H-8), 7.99–8.51 (m, 9H, Ar–H), 8.68 (s, 1H, triazole–H), 10.37 (s, 1H, NH). ESI-TOF *m*/*z* calcd (%) for $C_{30}H_{25}N_7O_4$ [M+Na]$^+$ 570.1860, found 570.1857.

4.5. 7-[2-Deoxy-5-*O*-(4,4′-dimethoxytrityl)-β-D-*erythro*-pentofuranosyl]-3,7-dihydro-2-(isobutyrylamino)-5-[1-(pyrenmethyl)-1*H*-1,2,3-triazol-4-yl]-4*H*-pyrrolo[2,3-*d*]pyrimidin-4-one (8)

To a solution of **7** (0.250 g, 0.38 mmol) and 1-azidomethylpyrene (0.146 g, 0.57 mmol) in THF/H_2O/*t*-BuOH (3:1:1, 5 mL), sodium ascorbate (0.83 mL, 0.84 mmol) of a freshly prepared 1 M solution in water and copper(II) sulfate pentahydrate 7.5% in water (0.76 mL, 0.23 mmol) were added. The reaction mixture was stirred vigorously in the dark at room temperature for 1 h and was monitored by TLC. After completion of the reaction, the solvent was evaporated, and the residue was purified by FC (silica gel, column 10 cm×3 cm, CH_2Cl_2/acetone, 85:15) to give **8** as a light yellow solid (0.236 g, 68%). TLC (CH_2Cl_2/acetone, 80:20): R_f 0.29; λ_{max} (MeOH)/nm 275 (ε/dm^3 mol^{-1} cm^{-1} 64,900), 311 (27,900), 325 (39,800), 342 (49,400). ^{1}H NMR (DMSO-d_6, 300 MHz) (δ, ppm): 1.09, 1.11 (2s, 6H, 2×CH_3), 2.19–2.23 (m, 1H, H$_\alpha$-2′), 2.50–2.51 (m, 1H, H$_\beta$-C2′), 2.70–2.76 (m, 1H, CH), 3.12–3.18 (m, 2H, 2×H-5′), 3.61, 3.64 (2s, 6H, 2×OCH_3), 3.90 (br s, 1H, H-4′), 4.31 (br s, 1H, H-3′), 5.33 (d, *J*=3.3 Hz, 1H, HO-3′), 6.41–6.45 (m, 3H, H-1′, CH_2), 6.79–6.82 (m, 4H, Ar–H), 7.06–7.35 (m, 9H, Ar–H), 7.66 (s, 1H, H-8), 8.07–8.56 (m, 9H, Pyr–H), 8.72 (s, 1H, triazole–H), 11.60 (s, 1H, NH), 11.82 (s, 1H, NH). Elemental analysis calcd (%) for $C_{55}H_{49}N_7O_7$ (920.02): C, 71.80; H, 5.37; N, 10.66. Found: C, 71.87; H, 5.36; N, 10.57.

4.6. 7-[2-Deoxy-5-*O*-(4,4′-dimethoxytrityl)-β-D-*erythro*-pentofuranosyl]-3,7-dihydro-2-(isobutyrylamino)-5-[1-(pyrenmethyl)-1*H*-1,2,3-triazol-4-yl]-4*H*-pyrrolo[2,3-*d*]pyrimidin-4-one 3′-(2-cyanoethyl)-*N*,*N*-diisopropylphosphoramidite (9)

To a solution of **8** (0.125 g, 0.14 mmol) in dry CH_2Cl_2 (10 mL), (*i*-Pr)$_2$NEt (0.044 g, 0.34 mmol) and 2-cyanoethyl-*N*,*N*-diisopropylphosphoramidochloridite (0.058 g, 0.24 mmol) were added. After stirring for 45 min at room temperature, the solution was diluted with CH_2Cl_2 (40 mL) and extracted with 5% aq $NaHCO_3$ solution (30 mL). The combined organic layer was dried over Na_2SO_4 and evaporated. The residue was purified by FC (silica gel, column 10×2 cm, CH_2Cl_2/acetone, 90:10) to give **9** as a colorless foam (0.097 g, 64%). TLC (CH_2Cl_2/acetone, 80:20): R_f 0.70. ^{31}P NMR ($CDCl_3$, 121 MHz) (δ, ppm): 147.8, 147.4. ESI-TOF *m*/*z* calcd (%) for $C_{64}H_{66}N_9O_8P$ [M+Na]$^+$ 1142.4664, found 1142.4628.

4.7. 1-[2-Deoxy-3′,5′-di-*O*-(*p*-toluoyl)-β-D-*erythro*-pentofuranosyl]-4-(pyrenyl)-1*H*-1,2,3-triazol-4-yl (12)

Compound **10**[23a] (0.250 g, 0.63 mmol) was dissolved in dry THF (9 mL) and degassed for 5 min with N_2. Then, 1-ethynylpyrene **11** (0.215 g, 0.95 mmol) was added, and both stirring and degassing were continued for another 5 min, followed by the addition of a freshly prepared 1 M solution of sodium ascorbate (190 μL, 0.19 mmol) in water and a 7.5% copper(II) sulfate solution in water (67 μL, 0.03 mmol). The final ratio of THF to H_2O in the reaction mixture was maintained as 3:1. Finally, *N*,*N*-diisopropylethylamine (DIPEA) was added to the reaction mixture (0.123 g, 0.95 mmol). The reaction mixture was refluxed at 80 °C overnight with stirring. The reaction mixture was evaporated and partitioned between water and dichloromethane. The organic layer was washed with water followed by brine solution, dried over Na_2SO_4, and concentrated. Then, the residue was purified by FC (silica gel, column 3×10 cm, CH_2Cl_2/EtOAc, 98:2) to give **12** as a colorless solid (0.327 g, 83%). TLC (CH_2Cl_2/EtOAc, 95:5): R_f 0.55; λ_{max} (MeOH)/nm 278 (ε/dm^3 mol^{-1} cm^{-1} 37,900), 346 (31,700). ^{1}H NMR (DMSO-d_6, 300 MHz) (δ, ppm): 2.22 (s, 3H, CH_3), 2.41 (s, 3H, CH_3), 2.97–3.06 (m, 1H, H$_\alpha$-2′), 3.35–3.44 (m, 1H, H$_\beta$-2′), 4.51–4.74 (m, 3H, 2×H-5′, H-4′), 5.88–5.93 (m, 1H, H-3′), 6.80 (t, *J*=6.0 Hz, 1H, H-1′), 7.18 (d, *J*=8.1 Hz, 2H, Ar–H), 7.38 (d, *J*=8.1 Hz, 2H, Ar–H), 7.85 (d, *J*=8.4 Hz, 2H, Ar–H), 7.98 (d, *J*=8.1 Hz, 2H, Ar–H), 8.09–8.38 (m, 8H, Ar–H), 8.80 (d, *J*=9.3 Hz, 1H, Ar–H), 8.98 (s, 1H, triazole-H). ESI-TOF *m*/*z* calcd (%) for $C_{39}H_{31}N_3O_5$ [M+Na]$^+$ 644.2156, found 644.2153.

4.8. 1-[2-Deoxy-β-D-*erythro*-pentofuranosyl]-4-(pyrenyl)-1*H*-1,2,3-triazol-4-yl (3)

A solution of **12** (0.326 g, 0.52 mmol) in THF (35 mL) and MeOH (0.35 mL) was treated with 1 M NaOMe in MeOH (0.099 g, 1.83 mmol). The reaction mixture was stirred overnight at room temperature, neutralized with acetic acid (106 μL), and evaporated to dryness under reduced pressure. Then, the residue was purified by FC (silica gel, column 3×10 cm, CH_2Cl_2/MeOH, 92:8) to give **3** as a colorless solid (0.182 g, 90%). TLC (CH_2Cl_2/MeOH, 90:10): R_f 0.35; λ_{max} (MeOH)/nm 260 (ε/dm^3 mol^{-1} cm^{-1} 16,100), 277 (39,300), 346 (31,700). ^{1}H NMR (DMSO-d_6, 300 MHz) (δ, ppm): 2.53–2.57 (m, 1H,

H_α-2′), 2.80–2.88 (m, 1H, H_β-2′), 3.52–3.69 (m, 2H, 2×H-5′), 3.97–3.98 (m, 1H, H-4′), 4.52 (br s, 1H, H-3′), 5.01 (t, J=5.4 Hz, 1H, OH-5′), 5.45 (d, J=4.2 Hz, 1H, OH-3′), 6.56 (t, J=5.7 Hz, 1H, H-1″), 8.08–8.39 (m, 8H, Ar–H), 8.85 (d, J=9.3 Hz, 1H, Ar–H), 8.95 (s, 1H, triazole–H). ESI-TOF m/z calcd (%) for (%) $C_{23}H_{19}N_3O_3$ $[M+Na]^+$ 408.1319, found 408.1314.

4.9. 1-[2-Deoxy-5-*O*-(4,4′-dimethoxytrityl)-β-D-*erythro*-pentofuranosyl]-4-(pyrenyl)-1*H*-1,2,3-triazol-4-yl (13)

Compound **3** (0.160 g, 0.41 mmol) was co-evaporated with anhydrous pyridine (3×8 mL) before dissolving in anhydrous pyridine (5 mL). Subsequently, 4,4′-dimethoxytrityl chloride (0.281 g, 0.83 mmol) and *N*,*N*-diisopropylethylamine (0.080 g, 0.62 mmol) were added. Then, the reaction mixture was stirred for 16 h at room temperature. After completion of reaction (TLC monitoring), the solvent was evaporated to dryness. To remove traces of pyridine, the residue was co-evaporated with toluene (10 mL). The residue was purified by FC (silica gel, column 3×10 cm, CH_2Cl_2/acetone, 95:5), to afford compound **13** (0.152 g, 53%) as a light yellow solid. TLC (CH_2Cl_2/acetone, 90:10): R_f 0.31; λ_{max} (MeOH)/nm 278 (ε/dm^3 mol^{-1} cm^{-1} 35,100), 346 (26,800). ^{1}H NMR (DMSO-d_6, 300 MHz) (δ, ppm): 2.51–2.60 (m, 1H, H_α-2′), 2.90–2.98 (m, 1H, H_β-2′), 3.17 (d, J=4.5 Hz, 2H, 2×H-5′), 3.50 (s, 3H, CH_3), 3.57 (s, 3H, CH_3), 4.06–4.11 (m, 1H, H-4′), 4.56–4.62 (m, 1H, H-3′), 5.49 (d, J=4.8 Hz, 1H, OH-3′), 6.59 (dd, J=4.2, 6.9 Hz, 1H, H-1′), 6.72–6.78 (m, 4H, Ar–H), 7.08–7.35 (m, 9H, Ar–H), 8.08–8.35 (m, 8H, Ar–H), 8.79 (d, J=9.3 Hz, 1H, Ar–H), 8.86 (s, 1H, triazole–H). ESI-TOF m/z calcd (%) for $C_{44}H_{37}N_3O_5$ $[M+Na]^+$ 710.2625, found 710.2620.

4.10. 1-[2-Deoxy-5-*O*-(4,4′-dimethoxytrityl)-β-D-*erythro*-pentofuranosyl]-4-(pyrenyl)-1*H*-1,2,3-triazol-4-yl 3′-(2-cyanoethyl)-*N*,*N*-diisopropylphosphoramidite (14)

To a solution of **13** (0.110 g, 0.16 mmol) in dry CH_2Cl_2 (8 mL), (*i*-Pr)$_2$NEt (0.052 g, 0.40 mmol) and 2-cyanoethyl *N*,*N*-diisopropylphosphoramidochloridite (0.068 g, 0.29 mmol) were added. After stirring for 30 min at room temperature, the solution was diluted with CH_2Cl_2 (30 mL) and extracted with 5% aq $NaHCO_3$ solution (20 mL), the combined organic layer was dried over Na_2SO_4 and evaporated. The residue was purified by FC (silica gel, column 10×2 cm, CH_2Cl_2/acetone, 95:5) to give **14** as a colorless foam (0.108 g, 76%). TLC (CH_2Cl_2/acetone, 90:10): R_f 0.62. ^{31}P NMR ($CDCl_3$, 121 MHz) (δ, ppm): 149.0, 149.4. ESI-TOF m/z calcd (%) for $C_{53}H_{54}N_5O_6P$ $[M+Na]^+$ 910.3704, found 910.3676.

4.11. 2-Amino-4-chloro-7-[2-deoxy-3′,5′-di-*O*-(*p*-toluoyl)-β-D-*erythro*-pentofuranosyl]-3,7-dihydro-4*H*-pyrrolo[2,3-*d*]pyrimidine (17)

To a suspension of powdered KOH (3.47 g, 61.8 mmol) in 500 mL acetonitrile was added compound **15**[28] (5.9 g, 35.0 mmol). After the reaction mixture was kept stirring for 5 min, compound **16**[29] (16.33 g, 42.0 mmol) was added within 5 min, and the mixture was stirred for another 15 min. Insoluble material was filtered off, the precipitate was washed with CH_2Cl_2 (10 mL), and the combined filtrate was evaporated to dryness. Purification by FC (silica gel, column 12×20 cm, CH_2Cl_2/MeOH, 98:2) gave **17** as a colorless foam (13.9 g, 76%). TLC (CH_2Cl_2/MeOH, 98:2): R_f 0.24. ^{1}H NMR (DMSO-d_6, 300 MHz) (δ, ppm): 2.37, 2.40 (2s, 6H, 2×CH_3), 2.61–2.68 (m, 1H, H_α-2′), 2.94–3.04 (m, 1H, H_β-2′), 4.47–4.63 (m, 3H, 2×H-5′, H-4′), 5.67 (d, J=6.0 Hz, 1H, H-3′), 6.38 (d, J=3.9 Hz, 1H, H-7), 6.55 (dd, J=5.7, 8.7 Hz, 1H, H-1′), 6.80 (s, 2H, NH_2), 7.31–7.39 (m, 5H, H-8, 4×ArH), 7.87–7.95 (m, 4H, 4×ArH). The obtained NMR data correspond to earlier reported literature values.[30]

4.12. 2-Amino-7-(2-deoxy-β-D-*erythro*-pentofuranosyl)-3,7-dihydro-5-iodo-4-methoxy-4*H*-pyrrolo[2,3-*d*]pyrimidine (19)

Compound **18**[31] (2.0 g, 2.79 mmol) was dissolved in 0.5 M CH_3ONa in methanol (75 mL) under heating and the reaction mixture was refluxed for 5 h. After completion of the reaction (TLC monitoring), the solvent was evaporated and the residue was purified by FC (silica gel, column 10×3 cm, CH_2Cl_2/MeOH, 95:5) to give **19** as a colorless solid (1.058 g, 93%). TLC (CH_2Cl_2/MeOH, 90:10): R_f 0.54. ^{1}H NMR (DMSO-d_6, 300 MHz) (δ, ppm): 2.02–2.09 (m, 1H, H_α-2′), 2.31–2.40 (m, 1H, H_β-2′), 3.46–3.51 (m, 2H, H-5′), 3.75–3.77 (m, 2H, H-4′), 3.91 (s, 3H, OCH_3), 4.26–4.27 (m, 1H, H-3′), 4.91 (t, J=5.4 Hz, 1H, OH-5′), 5.20 (d, J=3.6 Hz, 1H, OH-3′), 6.34–6.39 (m, 3H, H-1′, NH_2), 7.28 (s, 1H, H-8). The obtained NMR data correspond to earlier reported literature values.[32]

4.13. 2-Amino-7-(2-deoxy-β-D-*erythro*-pentofuranosyl)-3,7-dihydro-5-iodo-4*H*-pyrrolo[2,3-*d*]pyrimidin-4-one (20)

A suspension of compound **19** (1.0 g, 2.46 mmol) in 2 N NaOH (50 mL) was refluxed for 5 h. The solution was neutralized with acetic acid and the product was collected by filtration, washed with water, and dried to give **20** as a colorless solid (0.875 g, 91%). TLC (CH_2Cl_2/MeOH, 90:10): R_f 0.24. ^{1}H NMR (DMSO-d_6, 300 MHz) (δ, ppm): 2.01–2.07 (m, 1H, H_α-2′), 2.25–2.34 (m, 1H, H_β-2′), 3.43–3.52 (m, 2H, H-5′), 3.73 (br s, 1H, H-4′), 4.23 (br s, 1H, H-3′), 4.89 (t, J=5.4 Hz, 1H, OH-5′), 5.18 (d, J=3.3 Hz, 1H, OH-3′), 6.23–6.31 (m, 3H, H-1′, NH_2), 7.10 (s, 1H, H-8), 10.45 (s, 1H, NH). The obtained NMR data correspond to earlier reported literature values.[24]

4.14. 2-Amino-7-(2-deoxy-β-D-*erythro*-pentofuranosyl)-5-[2-(1-ethynylpyrenyl)]-3,7-dihydro-4*H*-pyrrolo[2,3-*d*]pyrimidin-4-one (4)

To a suspension of **20** (1.0 g, 2.55 mmol) and CuI (0.097 g, 0.51 mmol) in anhydrous DMF (15 mL) were added successively $[Pd(PPh_3)_4]$ (0.589 g, 0.51 mmol), anhydrous Et_3N (0.619 g, 6.12 mmol) and 1-ethynylpyrene (0.865 g, 3.82 mmol). The reaction mixture was stirred under nitrogen atmosphere and allowed to proceed until the starting material was consumed (TLC monitoring). The combined filtrate was evaporated, the residue was adsorbed on silica gel and subjected to FC (silica gel, column 15×4 cm, CH_2Cl_2/MeOH, 93:7) to give **4** as a light yellow solid (0.86 g, 69%). TLC (CH_2Cl_2/MeOH, 90:10): R_f 0.23; λ_{max} (MeOH)/nm 260 (ε/dm^3 mol^{-1} cm^{-1} 26,200), 285 (33,300), 389 (38,100). ^{1}H NMR (DMSO-d_6, 300 MHz) (δ, ppm): 2.13–2.21 (m, 1H, H_α-2′), 2.39–2.46 (m, 1H, H_β-2′), 3.55–3.60 (m, 2H, 2×H-5′), 3.81–3.84 (m, 1H, H-4′), 4.35–4.36 (m, 1H, H-3′), 5.01 (t, J=5.4 Hz, 1H, HO-5′), 5.29 (d, J=3.9 Hz, 1H, HO-3′), 6.38 (dd, J=5.7, 8.1 Hz, 1H, H-1′), 6.49 (s, 2H, NH_2), 7.58 (s, 1H, H-8), 8.08–8.37 (m, 8H, Pyr–H), 8.97 (d, J=9.0 Hz, 1H, Pyr–H), 10.62 (s, 1H, NH). ESI-TOF m/z calcd (%) for $C_{29}H_{22}N_4O_4$ $[M+Na]^+$ 513.1533, found 513.1531.

4.15. 7-[2-Deoxy-3′,5′-di-*O*-(*p*-toluoyl)-β-D-*erythro*-pentofuranosyl]-5-iodo-2-(isobutyrylamino)-3,7-dihydro-4*H*-pyrrolo[2,3-*d*]pyrimidin-4-one (21)

A solution of compound **18**[31] (1.2 g, 1.67 mmol), pyridine-2-carboxaldoxime (1.022 g, 8.37 mmol) and 1,1,3,3-tetramethylguanidine (0.964 g, 8.37 mmol) in a mixture of dioxane (19 mL) and DMF (21 mL) was stirred for 20 h under argon atmosphere at room temperature. The reaction mixture was diluted with ethyl acetate (100 mL) and washed with 5% HCl (100 mL), satd $NaHCO_3$ (100 mL), and brine (50 mL), dried over Na_2SO_4, and evaporated to dryness under reduced pressure. Purification by FC (silica gel, column 10×3 cm, CH_2Cl_2/EtOAc, 95:5) gave **21** as

a colorless solid (1.075 g, 92%). TLC (CH_2Cl_2/EtOAc, 95:5): R_f 0.17; λ_{max} (MeOH)/nm 296 (ε/dm^3 mol^{-1} cm^{-1} 13,700). ^{1}H NMR (DMSO-d_6, 300 MHz) (δ, ppm): 1.07, 1.16 (2s, 6H, 2×CH_3), 2.36, 2.37 (2s, 6H, 2×CH_3), 2.60–2.72 (m, 2H, CH, H_α-2′), 2.86–2.89 (m, 1H, H_β-2′), 4.47–4.58 (m, 3H, H-4′, 2×H-5′), 5.63 (d, J=5.4 Hz, 1H, H-3′), 6.45 (dt, J=6.0, 8.7 Hz, 1H, H-1′), 7.30–7.38 (m, 5H, H-8, 4×Ar–H), 7.85–7.91 (m, 4H, Ar–H), 11.49 (s, 1H, NH), 11.79 (s, 1H, NH). Elemental analysis calcd (%) for $C_{31}H_{31}IN_4O_7$ (698.50): C, 53.30; H, 4.47; N, 8.02. Found C, 53.54; H, 4.71; N, 7.93.

4.16. 7-[2-Deoxy-β-D-*erythro*-pentofuranosyl]-5-iodo-2-(isobutyrylamino)-3,7-dihydro-4*H*-pyrrolo[2,3-*d*]pyrimidin-4-one (22)

A solution of compound **21** (1.075 g, 1.54 mmol) in THF (35 mL) and methanol (0.35 mL) was treated with 1 M NaOMe in MeOH (3.07 mL, 3.08 mmol) at 0 °C in an ice-bath. The ice-bath was removed and stirring was continued at room temperature. After completion of the reaction (TLC monitoring), the reaction mixture was neutralized with acetic acid (0.19 mL) and evaporated to dryness under reduced pressure. Purification by FC (silica gel, column 10×3 cm, CH_2Cl_2/MeOH, 95:5) gave **22** as a colorless solid (0.637 g, 90%). TLC (CH_2Cl_2/MeOH, 90:10): R_f 0.32. ^{1}H NMR (DMSO-d_6, 300 MHz) (δ, ppm): 1.10, 1.12 (2s, 6H, 2×CH_3), 2.08–2.15 (m, 1H, H_α-2′), 2.35–2.42 (m, 1H, H_β-2′), 2.69–2.78 (m, 1H, CH), 3.46–3.55 (m, 2H, H-5′), 3.76–3.80 (m, 1H, H-4′), 4.30–4.31 (m, 1H, H-3′), 4.93 (t, J=5.4 Hz, 1H, OH-5′), 5.24 (d, J=3.0 Hz, 1H, OH-3′), 6.36 (dt, J=5.7, 8.4 Hz, 1H, H-1′), 7.45 (s, 1H, H-8), 11.55 (s, 1H, NH), 11.78 (s, 1H, NH). The obtained NMR data correspond to earlier reported literature values.[27]

4.17. 7-[2-Deoxy-5-*O*-(4,4′-dimethoxytrityl)-β-D-*erythro*-pentofuranosyl]-5-[2-(1-ethynylpyrenyl)]-3,7-dihydro-2-(isobutyrylamino)-4*H*-pyrrolo[2,3-*d*]pyrimidin-4-one (24)

To a suspension of **23** (0.385 g, 0.50 mmol) and CuI (0.019 g, 0.10 mmol) in anhydrous DMF (5 mL) were added successively [Pd(PPh_3)$_4$] (0.058 g, 0.05 mmol), anhydrous Et_3N (0.122 g, 1.21 mmol), and 1-ethynylpyrene (0.171 g, 0.76 mmol). The reaction mixture was stirred under nitrogen atmosphere and allowed to proceed until the starting material was consumed (TLC monitoring). The combined filtrate was evaporated, the residue was adsorbed on silica gel and subjected to FC (silica gel, column 10×3 cm, CH_2Cl_2/acetone, 95:5) to give **24** as a light yellow solid (0.308 g, 71%). TLC (CH_2Cl_2/acetone, 90:10): R_f 0.35; λ_{max} (MeOH)/nm 288 (ε/dm^3 mol^{-1} cm^{-1} 36,700), 389 (40,700). ^{1}H NMR (DMSO-d_6, 300 MHz) (δ, ppm): 1.14, 1.16 (2s, 6H, 2×CH_3), 2.28–2.35 (m, 1H, H_α-2′), 2.59–2.65 (m, 1H, H_β-C2′), 2.77–2.82 (m, 1H, CH), 3.12–3.20 (m, 2H, 2×H-5′), 3.64, 3.65 (2s, 6H, 2×OCH_3), 3.96 (br s, 1H, H-4′), 4.42 (br s, 1H, H-3′), 5.38 (d, J=3.6 Hz, 1H, HO-3′), 6.48 (t, J=6.4 Hz, 1H, H-1′), 6.84–6.88 (m, 4H, Ar–H), 7.16–7.41 (m, 9H, Ar–H), 7.76 (s, 1H, H-8), 8.10–8.39 (m, 8H, Ar–H), 8.90 (d, J=9.0 Hz, 1H, Ar-H), 11.69 (s, 1H, NH), 12.04 (s, 1H, NH). Elemental analysis calcd (%) for $C_{54}H_{46}N_4O_7$ (862.97): C, 75.16; H, 5.37; N, 6.49. Found: C, 75.32; H, 5.40; N, 6.50.

4.18. 7-[2-Deoxy-5-*O*-(4,4′-dimethoxytrityl)-β-D-*erythro*-pentofuranosyl]-5-[2-(1-ethynylpyrenyl)]-3,7-dihydro-2-(isobutyrylamino)-4*H*-pyrrolo[2,3-*d*]pyrimidin-4-one 3′-(2-cyanoethyl)-*N*,*N*-diisopropylphosphoramidite (25)

To a solution of **24** (0.180 g, 0.21 mmol) in dry CH_2Cl_2 (10 mL), (*i*-Pr)$_2$NEt (0.067 g, 0.52 mmol) and 2-cyanoethyl *N*,*N*-diisopropylphosphoramidochloridite (0.089 g, 0.38 mmol) were added. After stirring for 45 min at room temperature, the solution was diluted with CH_2Cl_2 (40 mL) and extracted with 5% aq $NaHCO_3$ solution (30 mL). The combined organic layer was dried over Na_2SO_4 and evaporated. The residue was purified by FC (silica gel, column 10×2 cm, CH_2Cl_2/acetone, 95:5) to give **25** as a colorless foam (0.160 g, 72%). TLC (CH_2Cl_2/acetone, 90:10): R_f 0.75. ^{31}P NMR ($CDCl_3$, 121 MHz) (δ, ppm): 148.2, 147.5. ESI-TOF *m*/*z* calcd (%) for $C_{63}H_{63}N_6O_8P$ $[M+Na]^+$ 1085.4337, found 1085.4320.

Acknowledgements

We thank Dr. S. Budow-Busse and Dr. P. Leonard for helpful discussions and support while preparing the manuscript. We also thank Mr. S.S. Pujari and H. Mei for measuring the NMR spectra and Mr. Nhat Quang Tran for the oligonucleotide syntheses. We would like to thank Dr. M. Letzel, Organisch-Chemisches Institut, Universität Münster, Germany, for the measurement of the MALDI spectra. Financial support by ChemBiotech, Münster, Germany, is highly appreciated.

Supplementary data

^{1}H–^{13}C coupling constants, HPLC profiles, additional UV–vis and fluorescence spectra, fluorescence brightness values, monomer to excimer fluorescence ratios, copies of ^{1}H, ^{13}C NMR, DEPT-135, and ^{1}H–^{13}C gated-decoupled NMR spectra. Supplementary data associated with this article can be found in the online version, at http://dx.doi.org/10.1016/j.tet.2013.11.048.

References and notes

1. (a) Förster, T.; Kasper, K. *Z. Elektrochem.* **1955**, *59*, 976; (b) Birks, J. B. *Photophysics of Aromatic Molecules*; Wiley-Interscience: London, UK, 1970; (c) Birks, J. B. *Org. Mol. Photophys.* **1975**, *2*, 409.
2. (a) Kalyanasundaram, K.; Thomas, J. K. *J. Am. Chem. Soc.* **1977**, *99*, 2039; (b) Bag, S. S.; Kundu, R.; Matsumoto, K.; Saito, Y.; Saito, I. *Bioorg. Med. Chem. Lett.* **2010**, *20*, 3227.
3. Birks, J. B. *Rep. Prog. Phys.* **1975**, *38*, 903.
4. Winnik, F. M. *Chem. Rev.* **1993**, *93*, 587.
5. Bains, G.; Patel, A. B.; Narayanaswami, V. *Molecules* **2011**, *16*, 7909.
6. Sahoo, D.; Narayanaswami, V.; Kay, C. M.; Ryan, R. O. *Biochemistry* **2000**, *39*, 6594.
7. (a) Wang, G.; Bobkov, G. V.; Mikhailov, S. N.; Schepers, G.; Van Aerschot, A.; Rozenski, J.; Van der Auweraer, M.; Herdewijn, P.; De Feyter, S. *ChemBioChem* **2009**, *10*, 1175; (b) Mansawat, W.; Boonlua, C.; Siriwong, K.; Vilaivan, T. *Tetrahedron* **2012**, *68*, 3988; (c) Werder, S.; Malinovskii, V. L.; Häner, R. *Org. Lett.* **2008**, *10*, 2011; (d) Dioubankova, N. N.; Malakhov, A. D.; Shenkarev, Z. O.; Korshun, V. A. *Tetrahedron* **2004**, *60*, 4617; (e) Grünewald, C.; Kwon, T.; Piton, N.; Förster, U.; Wachtveitl, J.; Engels, J. W. *Bioorg. Med. Chem.* **2008**, *16*, 19.
8. (a) Østergaard, M. E.; Hrdlicka, P. J. *Chem. Soc. Rev.* **2011**, *40*, 5771; (b) Karlsen, K. K.; Pasternak, A.; Jensen, T. B.; Wengel, J. *ChemBioChem* **2012**, *13*, 590; (c) Wagner, C.; Rist, M.; Mayer-Enthart, E.; Wagenknecht, H.-A. *Org. Biomol. Chem.* **2005**, *3*, 2062; (d) Wojciechowski, F.; Lietard, J.; Leumann, C. J. *Org. Lett.* **2012**, *14*, 5176; (e) Honcharenko, D.; Zhou, C.; Chattopadhyaya, J. *J. Org. Chem.* **2008**, *73*, 2829.
9. (a) Tanhuanpää, K.; Virtanen, J.; Somerharju, P. *Biochim. Biophys. Acta* **2000**, *1497*, 308; (b) Baek, Y.-K.; Jung, D.-H.; Yoo, S. M.; Shin, S.; Kim, J.-H.; Jeon, H.-J.; Choi, Y.-K.; Lee, S. Y.; Jung, H.-T. *J. Nanosci. Nanotechnol.* **2011**, *11*, 4210.
10. Seela, F.; He, Y.; Wei, C. *Tetrahedron* **1999**, *55*, 9481.
11. Guckian, K. M.; Schweitzer, B. A.; Ren, R. X.-F.; Sheils, C. J.; Tahmassebi, D. C.; Kool, E. T. *J. Am. Chem. Soc.* **2000**, *122*, 2213.
12. (a) Sau, S. P.; Hrdlicka, P. J. *J. Org. Chem.* **2012**, *77*, 5; (b) Christensen, U. B.; Pedersen, E. B. *Helv. Chim. Acta* **2003**, *86*, 2090.
13. (a) Ingale, S. A.; Pujari, S. S.; Sirivolu, V. R.; Ding, P.; Xiong, H.; Mei, H.; Seela, F. *J. Org. Chem.* **2012**, *77*, 188; (b) Mei, H.; Ingale, S. A.; Seela, F. *Tetrahedron* **2013**, *69*, 4731; (c) Seela, F.; Ingale, S. A. *J. Org. Chem.* **2010**, *75*, 284.
14. Okamoto, A.; Kanatani, K.; Saito, I. *J. Am. Chem. Soc.* **2004**, *126*, 4820.
15. (a) Seo, Y. J.; Hwang, G. T.; Kim, B. H. *Tetrahedron Lett.* **2006**, *47*, 4037; (b) Hwang, G. T.; Seo, Y. J.; Kim, B. H. *Tetrahedron Lett.* **2005**, *46*, 1475.
16. (a) Malinovskii, V. L.; Wenger, D.; Häner, R. *Chem. Soc. Rev.* **2010**, *39*, 410; (b) Wang, C.; Wu, C.; Chen, Y.; Song, Y.; Tan, W.; Yang, C. J. *Curr. Org. Chem.* **2011**, *15*, 465; (c) Venkatesan, N.; Seo, Y. J.; Bang, E. K.; Park, S. M.; Lee, Y. S.; Kim, B. H. *Bull. Korean Chem. Soc.* **2006**, *27*, 613; (d) Teo, Y. N.; Kool, E. T. *Chem. Rev.* **2012**, *112*, 4221.
17. Mayer, E.; Valis, L.; Wagner, C.; Rist, M.; Amann, N.; Wagenknecht, H.-A. *ChemBioChem* **2004**, *5*, 865.
18. (a) Malakhov, A. D.; Malakhova, E. V.; Kuznitsova, S. V.; Grechishnikova, I. V.; Prokhorenko, I. A.; Skorobogatyi, M. V.; Korshun, V. A.; Berlin, Y. A. *Russ. J. Bioorg. Chem.* **2000**, *26*, 34; (b) Gaballah, S. T.; Netzel, T. L. *Heterocycl. Commun.* **2005**, *11*, 241; (c) Hwang, G. T.; Seo, Y. J.; Kim, S. J.; Kim, B. H. *Tetrahedron Lett.*

2004, *45*, 3543; (d) Østergaard, M. E.; Guenther, D. C.; Kumar, P.; Baral, B.; Deobald, L.; Paszczynski, A. J.; Sharma, P. K.; Hrdlicka, P. J. *Chem. Commun.* **2010**, 4929; (e) Okamoto, A.; Ochi, Y.; Saito, I. *Chem. Commun.* **2005**, 1128; (f) Seo, Y. J.; Ryu, J. H.; Kim, B. H. *Org. Lett.* **2005**, *7*, 4931.
19. Saito, Y.; Miyauchi, Y.; Okamoto, A.; Saito, I. *Chem. Commun.* **2004**, 1704.
20. (a) Huisgen, R.; Szeimies, G.; Möbius, L. *Chem. Ber.* **1967**, *100*, 2494; (b) Tornøe, C. W.; Christensen, C.; Meldal, M. *J. Org. Chem.* **2002**, *67*, 3057; (c) Rostovtsev, V. V.; Green, L. G.; Fokin, V. V.; Sharpless, K. B. *Angew. Chem., Int. Ed.* **2002**, *41*, 2596; (d) Seela, F.; Sirivolu, V. R. *Chem. Biodivers.* **2006**, *3*, 509; (e) Kiviniemi, A.; Virta, P.; Lönnberg, H. *Bioconjugate Chem.* **2008**, *19*, 1726.
21. (a) Neef, A. B.; Samain, F.; Luedtke, N. W. *ChemBioChem* **2012**, *13*, 1750; (b) Ingale, S. A.; Mei, H.; Leonard, P.; Seela, F. *J. Org. Chem.* **2013**, *78*, 1127, http://dx.doi.org/10.1021/jo401780u
22. Park, S. Y.; Yoon, J. H.; Hong, C. S.; Souane, R.; Kim, J. S.; Matthews, S. E.; Vicens, J. *J. Org. Chem.* **2008**, *73*, 8212.
23. (a) Štimac, A.; Kobe, J. *Carbohydr. Res.* **2000**, *329*, 317; (b) St. Amant, A. H.; Bean, L. A.; Guthrie, J. P.; Hudson, R. H. E. *Org. Biomol. Chem.* **2012**, *10*, 6521.
24. Ramzaeva, N.; Seela, F. *Helv. Chim. Acta* **1995**, *78*, 1083.
25. (a) Seela, F.; Sirivolu, V. R.; Chittepu, P. *Bioconjugate Chem.* **2008**, *19*, 211; (b) Seela, F.; Shaikh, K. I. *Tetrahedron* **2005**, *61*, 2675; (c) Okamoto, A.; Taiji, T.; Tanaka, K.; Saito, I. *Tetrahedron Lett.* **2000**, *41*, 10035; (d) Dadová, J.; Vidláková, P.; Pohl, R.; Havran, L.; Fojta, M.; Hocek, M. *J. Org. Chem.* **2013**, *78*, 9627; (e) Saito, Y.; Suzuki, A.; Ishioroshi, S.; Saito, I. *Tetrahedron Lett.* **2011**, *52*, 4726.
26. (a) Buhr, C. A.; Wagner, R. W.; Grant, D.; Froehler, B. C. *Nucleic Acids Res.* **1996**, *24*, 2974; (b) Kazimierczuk, Z.; Cottam, H. B.; Revankar, G. R.; Robins, R. K. *J. Am. Chem. Soc.* **1984**, *106*, 6379.
27. Ramzaeva, N.; Seela, F. *Helv. Chim. Acta* **1996**, *79*, 1549.
28. Seela, F.; Kehne, A.; Winkeler, H.-D. *Liebigs Ann. Chem.* **1983**, 137.
29. Hoffer, M. *Chem. Ber.* **1960**, *93*, 2777.
30. Seela, F.; Westermann, B.; Bindig, U. *J. Chem. Soc., Perkin Trans. 1* **1988**, 697.
31. Angelov, T.; Guainazzi, A.; Schärer, O. D. *Org. Lett.* **2009**, *11*, 661.
32. Meng, Q.; Kim, D. H.; Bai, X.; Bi, L.; Turro, N. J.; Ju, J. *J. Org. Chem.* **2006**, *71*, 3248.
33. (a) Grabowski, Z. R.; Rotkiewicz, K.; Rettig, W. *Chem. Rev.* **2003**, *103*, 3899; (b) Fiebig, T.; Stock, K.; Lochbrunner, S.; Riedle, E. *Chem. Phys. Lett.* **2001**, *345*, 81.
34. (a) Kumar, P.; Shaikh, K. I.; Jørgensen, A. S.; Kumar, S.; Nielsen, P. *J. Org. Chem.* **2012**, *77*, 9562; (b) Wilson, J. N.; Teo, Y. N.; Kool, E. T. *J. Am. Chem. Soc.* **2007**, *129*, 15426.
35. Wagenknecht, H.-A. *Charge Transfer in DNA*; Wiley-VCH: Weinheim, Germany, 2005.
36. Seo, Y. J.; Rhee, H.; Joo, T.; Kim, B. H. *J. Am. Chem. Soc.* **2007**, *129*, 5244.
37. (a) Hrdlicka, P. J.; Babu, B. R.; Sørensen, M. D.; Wengel, J. *Chem. Commun.* **2004**, 1478; (b) Astakhova, I. V.; Malakhov, A. D.; Stepanova, I. A.; Ustinov, A. V.; Bondarev, S. L.; Paramonov, A. S.; Korshun, V. A. *Bioconjugate Chem.* **2007**, *18*, 1972.
38. Kaura, M.; Kumar, P.; Hrdlicka, P. J. *Org. Biomol. Chem.* **2012**, *10*, 8575.